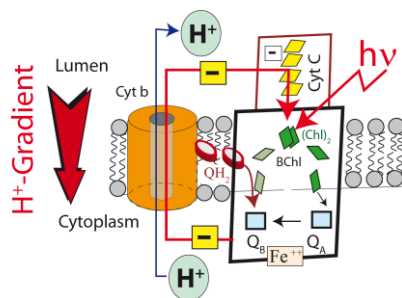
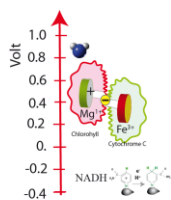


Erich Sackmann: Lecture Notes in Biophysics

Biomimetic Physics: Nature as nanomaterial designer and engineer.



Copyright Erich Sackmann, Physics Department Technical University Munich.

The text can be freely downloaded via the website: www.biophy.de.
Please cite as private communication

Erich Sackmann Lecture Notes

Biomimetic Physics: Nature as nanomaterial designer and engineer.

Erich Sackmann

Technical University Munich, Physics Department E22, James Franck Str.1
D85747 Garching, Germany. Email: sackmann @ph.tum.de

Abstract

The sheer infinite manifold of living beings has been designed with an astonishing small number of organic molecules. This was achieved by interplay of physics chemistry and genetics and the concept of hierarchical design. Many concepts of human rational design of smart materials have been invented by Mother Nature several billion years ago. Nature can teach us how to design highly sophisticated mechanical structures and systems comprising lengths scales from nanometer to meters by hierarchical design from functional modules (such as lipid membranes ion pumps, and molecular motors). Outstanding examples of primordial evolution are (i) the selection of smart organic molecular resulting in the self-assembly of energy producing machines, (ii) the advent of proton powered rotating motors enabling bacteria to search for food or escape dangers (iii) the design of smart materials exhibiting shape memory for rapid switching or unique surface properties. The design of larger animals from molecular modules was guided by the scaling laws of physics.

I. Introduction:

The main motivation of this talk is to introduce students of biophysics into the evolution of the sheer infinite manifold of living beings by interplay of physics genetics and biological control. The Development of new devices or biological concepts took place in quantum jumps which were driven by life threatening evolutionary crises. Intensive studies of these questions are expected to lead to

new strategies for solving major future challenges, including global chronic food shortage, global heating and even social conflicts. Of course we can never verify models or scenarios of biological evolution. However, the occupation with these fascinating questions stimulates the interdisciplinary cooperation and the education of a new generation of students who are better suited to solve future ecological crises than the present societies.

In this short contribution I will first concentrate on the selection of specific molecules, the development of transient electron storage devices and the concept of protomotoric force enabling the taming of organic chemical reactions during the prebiotic stage of evolution. In the second part I will show how nature invented new materials and made use of solid state phase transitions and shape memory effects enabling the survival of animals under harsh environmental conditions (say in the desert).

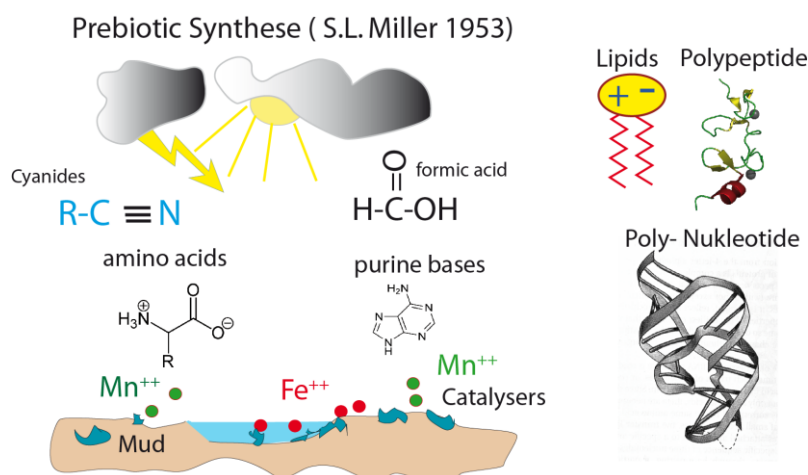


*Figure 1: A prebiotic scenario. Left: possible scenario of primordial soup (Ursuppe) 4 billion years ago; as suggested by the famous Miller-Urey experiments performed in the test tube. In mud stones and ponds many organic molecules could form from CO_2 , CO and methane generated by geothermal processes, such as formic acid cyanes and ammoniac by irradiation with UV-light and electric discharges. From these simple compounds amino acids and purine bases could form in the presence of heavy metal ions. Under mild conditions small poly-amino-acids and short DNA strands or polysaccharides can form by condensation reactions. For prebiotic formation of DNA-oligomers see M. Eigen, *Die Naturwissenschaften* **58**, 465-523 (1971).*

II. Nature as Physicochemist.

Development of transient electron storage molecules: Under the condition of the prebiotic state nature could most probably draw from an unlimited supply of different organic molecules, including sugar molecules, aromatic molecules, purine and pyrimidine bases, amino acids (but little oxygen). Evidence for this assumption came from the surprising and now very famous experiments of S. Miller, showing that in the presence of H_2 , CH_4 , H_2O , NH_3 , HCN many different small molecules such as amino acids (glycine, alanine), purine bases (uracil and glycine) can form from HCN under the action of light and electric discharges. Sugar molecules can form in aqueous solutions of formaldehyde by electric discharges and in the presence of lime. Other important early molecules were water soluble phosphate derivatives, such as phosphoric acid ($H_2PO_4^-$), which can easily form from metalphosphides such as Fe_3P . Triphosphates, the inorganic part of adenosine triphosphates (ATP), could then easily be formed by oxidation of $H_2PO_4^-$ [Pasek 2008]. Even the formation of DNA and Polypeptides has been observed in the presence of the heavy ions (Mn^{++}) as catalyzers.

A severe evolution crisis arising early on was the reversibility of chemical reactions in solution. The first step of evolution was the advent of methods to control the organic reactions in such a way that they become irreversible and to protect complex reaction products. In Organic Chemistry courses we learn that generation of organic molecules is always associated with transfer of electrons between precursor molecules through reduction and oxidation reactions. On the other side we also learn that free electrons are unstable in water. They live only about 10^{-8} sec as solvated electrons and their decay would destroy large biomolecules formed by chance such as DNA double helices by causing double strand breaks (the major fatal radiation damage in cells). This crisis was solved by two “inventions”: the fabrication of semipermeable shells (such as lipid membranes) and transient electron storage devices.

Proteins as electron caches and vesicles as zero model of cells.

Fig 1 shows the evolution of the electron cache (temporary storage device) cytochrome C about 3.5×10^9 years ago (or 1.5×10^9 years after the generation of the earth) which solved a fundamental problem. Most biochemical reactions, such as the splitting of oxygen O_2 by sunlight (associated with the formation of water) or the transformation of H_2O into O_2 in photosynthetic systems set free several free electrons. How could nature stabilize the free electrons to overcome the self-destruction of large organic molecules? Every chemist would tell you: search for a transient storage device which can capture electrons in such a way that they can be transferred to other reactants in a controllable way. He would further tell you first, to bind the electron to heavy metal ion (such as Iron Fe^{3+}

after the reaction: $\text{Fe}^{3+} + e^- \leftrightarrow \text{Fe}^{2+}$). To control the binding strength of the electrons he would advise you to embed the iron in organic molecules such as porphyrins and which often serves as catalyst in modern chemistry). By embedding the porphyrin catalyst in proteins nature finally generated confined reaction spaces in which processes such as electron transfer reactions can be controlled in subtle ways.

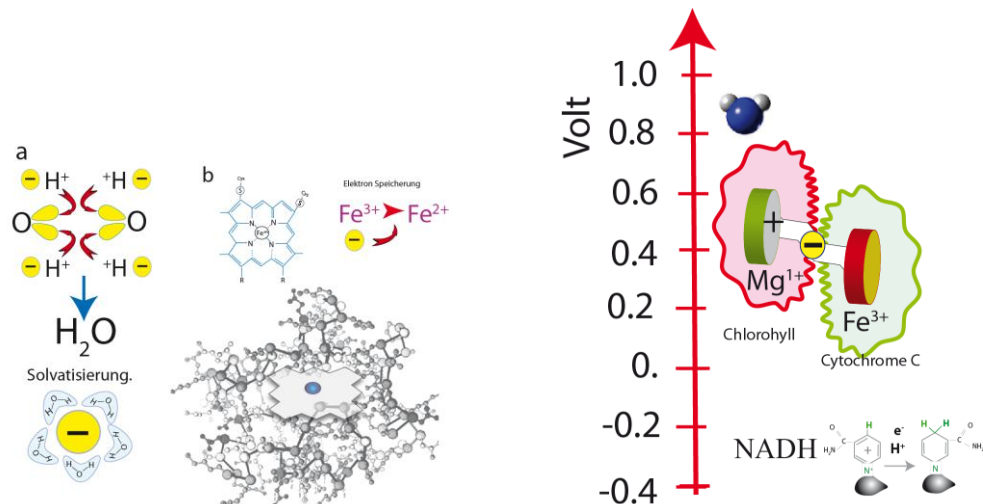


Figure 2

The taming of electron transfer reactions. (a) Schematic view of storage of electrons generated during the splitting of O_2 by binding to Fe^{3+} ions forming a coordinate bond with porphyrin. By changing the type of ion or the side groups of the porphyrin rings, the binding energy (measured in terms of eV) can be adjusted. To protect the molecular electron cache the metal porphyrin is embedded in proteins.

(b) The binding energy of electrons can be controlled by the type of metal, the side groups of the porphyrins (such as in chlorophyll a and b) or by using other types of electron carriers (such as quinones, NAD^+ or NADPH^+). NADPH is a reducing coenzyme which provides negatively charged hydrogen atoms (hydride ion) for the generation of hydrogen-rich molecules. To transfer electron from high to low energy states one can do chemical work. The figure shows a possible scenario for the cleavage of oxygen and the generation of the reducing agent NADPH. The reaction will proceed in the direction of decreasing energy.

An early evolutionary crisis triggered the development of proton pumps leading to the concept of protomotoric force generators

An essential step towards the development of living matter was the enclosure of the primitive molecular devices in lipid vesicles, generating protected reaction spaces with semi-permeable shells. In these, geo-thermally produced organic molecules could be used to produce NADPH, a basic co-enzyme, universally

used as reducing agent to produce hydrogen rich molecules. However, this constraint of reaction space provided two problems. First, the reactions were still reversible, due to strong temperature fluctuations and second, the pH could not be controlled impeding most biochemical reactions. This problem was overcome by separating the reaction products by semipermeable membranes and by the evolution of light driven proton pumps, such as bacteriorhodopsin of halobacteria (see Figure 3). By generating three reaction spaces the lumen the cytoplasm and the environment as in bacteria, the biochemical reactions could be controlled in subtle way.

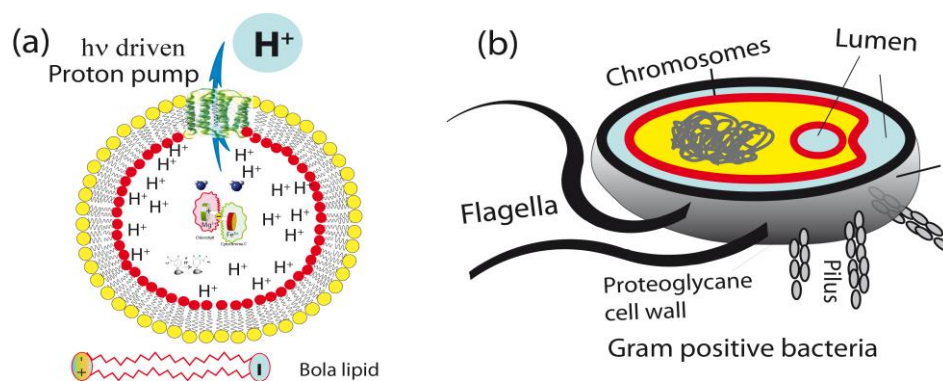


Figure 3: (a) Protection of primitive biochemical machines in vesicles enclosed by self-assembled lipid bilayer. The early bacteria were composed of bipolar bola lipids forming monolayers with low proton permeability. To avoid inhibition of reaction by low pH, the proton concentration is controlled by light driven proton pump embedded in the membrane. The pH could be adjusted self-consistently by coupling the pump activity to pH-gradient. (b) Design of bacteria with cell wall (gram positive) stressing the design by two semipermeable shells: the outer proteoglycan shell and the internal lipid/protein bilayer. The two walls generate three separate reaction spaces coupled by molecular exchange through semipermeable inner membranes. The function of the flagella as rotating motor is discussed below (see Figure 5).

Electron transfer reactions: Where quantum mechanics meets biology.

A frequently asked question is whether quantum physics plays a role in biology. One example is the generation of proton gradients by the photosystem of **purple bacteria**. It is simultaneously the most stunning invention in prebiotic evolution which paved the way for the universal methods of energy production by protomotoric forces in the ATP-synthase machine. Protomotoric forces can be generated by water splitting in algae and plants or in mitochondria by oxygen splitting, called oxidative phosphorylation.

In the present contribution we are interested in the physical basis of energy production and restrict the discussion to the proton gradient generation by cyclic

trans-membrane electron transfer in the purple bacteria [Deisenhofer]. The concept of ATP-production by oxygen splitting in mitochondria is summarized in the Appendix A.

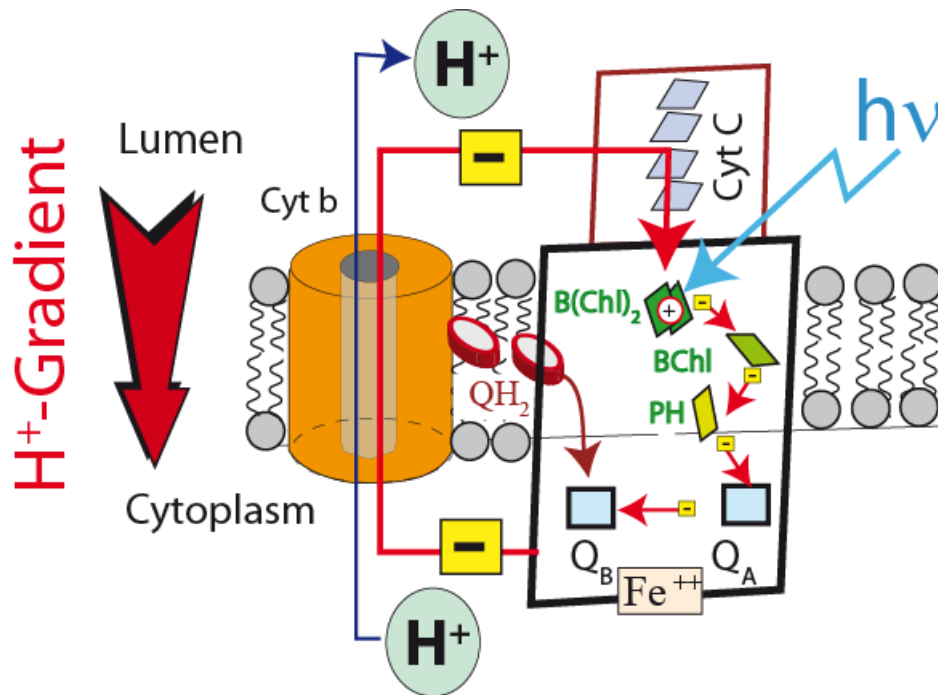


Figure 4.

Transformation of photon energy in protomotoric force by photosystem of purple bacteria through the cyclic trans-membrane electron transfer. Electrons are generated by photodissociation of the bacteriochlorophyll dimer ($B\text{-Chl}_2$). They flow over several redox partners (a chlorophyll monomer, pheophytin and two quinones (see Glossar)) to the electron acceptor Cytochrom C (Cyt C) as shown by the red arrow. The electron flow is associated with a proton flux generating the proton motoric force. The electron cache Cyt C can store several electrons and deliver them one by one to the electron hole generated in $B\text{-Chl}_2$ by photo-dissociation.

The protomotoric force generation in mitochondria could only evolve after the production of oxygen by photosynthetic systems of cyanobacteria and algae around 2 billion years ago. This great evolutionary step was preceded by the generation of proton gradients by more primitive photosystems of purple bacteria. Studies of fossils suggest that this membrane-bound and light-driven proton pump, shown in Figure 4, developed about $3.4 \cdot 10^9$ years ago. Electrons are generated by photo-dissociation of the chlorophyll dimer ($B\text{-Chl}_2$) (acting as primary electron donor) and jump over several redox partners down the energy ladder to the electron acceptor plastochinone. This stable, energy rich electron acceptor binds the electron together with a proton and delivers it to the

membrane bound redox-system cytochrome b. From here the electrons are taken over by the cytochrome C, which has a much higher electron affinity. A unique feature of this cytochrome C is that it has four porphyrin groups and can bind more than one electron. Therefore, the electron hole generated in the primary electron donor B-Chl₂ is filled up again by one of these stored electrons. The unique role of this cyclic electron flow across the membrane is to generate a proton gradient. Thus it appears that the primary energy source of biology was the proton gradient and not ATP. By the evolution of the ATP synthase the bacteria could survive by exploiting the geothermal energy (say CH₄). However, a quantum jump of evolution occurred with advent of the water splitting photosystems of algae and plants, which is not considered here.

How nature controls chemical stoichiometry and uses quantum physics.

Nature had to find solutions to fulfill the stoichiometric laws of chemistry.

Water or oxygen splitting delivers simultaneously several electrons while only one elementary charge is needed to neutralize the electron hole generated in the Chlorophyll dimer (B-Chl)₂ after each photon absorption and dissociation event. Nature found several solutions to solve this problem:

- One is shown Figure 4. The specific cytochrome C of the reaction center can reversibly bind one electron at each porphyrin. Since the ionized chlorophyll B-Chl⁺ is a very strong oxidant it withdraws its missing electron from the pool in cytochrome C.

- Other unique electron buffers which can simultaneously bind two electrons and release them one-by-one are the quinone derivatives. By uptake of one electron they form the stable free radical semi-quinone while hydro-quinone is formed after binding of the second one (see Appendix A). As shown in Figure 4 these molecules serve the transport of electrons from the chlorophyll dimer to the cytochrome b protein in the photosystem. A major advantage of quinones is that they can very effectively transport single electrons within membranes. Their diffusion coefficient is about $D \sim 10^{-7} \text{ cm}^2 \text{ sec}^{-1}$, that is they can move over distances of 1 μm within 1 sec.

- In the case of water splitting in photosynthetic systems an electron buffer which can simultaneously take up all 4 electrons and deliver them one to one to the electron hole in chlorophyll was needed. Nature found the solution with manganese complexes shown in Figure 5a. In these complexes of algamate type four manganese ions can store one electron. In the ground state these chelates contain four Mn³⁺-ions forming stable complexes with the oxygen groups. In fact, the selection of manganese was a smart choice. It is an element which can change the oxygenation state from -7 to + 7, whereby Mn³⁺ is the most stable state. In photosynthetic systems of plants, the complex is embedded in a protein coupled to the reaction center. The dissociated chlorophylls (Chl)⁺ withdraws single electrons from the Mn³⁺-ions which go over into Mn⁴⁺. After four such events the complex simultaneously withdraws four electrons from the complex

generating two oxygen molecules (see [Renger 2007] and [Sackmann/Merkel 2009]).

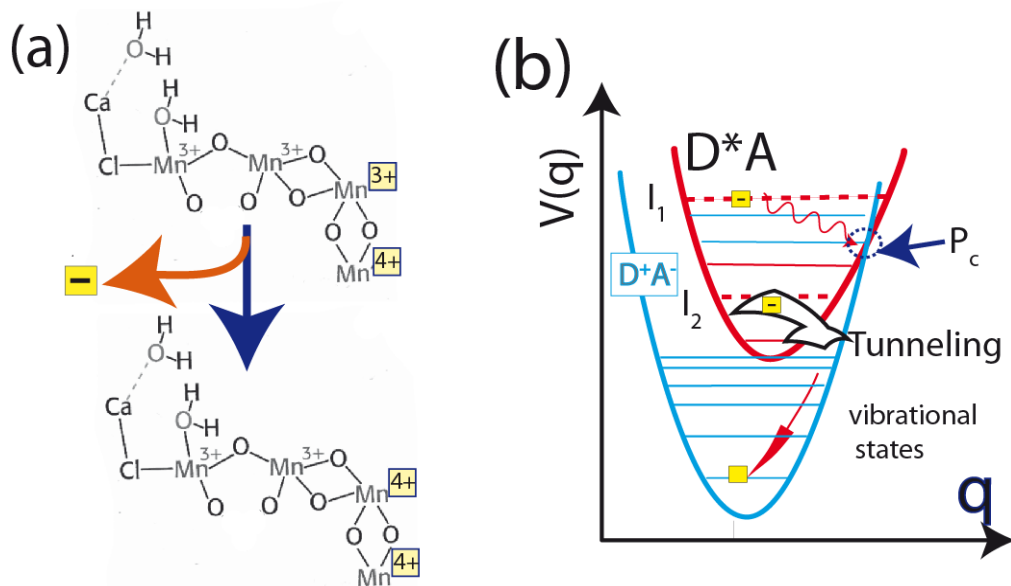


Figure 5

(a) Structure of manganese-chelate of algamate type, an electron buffer which can simultaneously take up all 4 electrons from water and deliver them one-by-one to the electron hole of chlorophyll. In the ground state, all ions are threefold charged. The two-fold oxidized state is shown where two electrons have been delivered to the electron acceptor (such as the defect electron in chlorophyll).

(b) Charge separation by transition of electron from the excited donor D^* to the acceptor A in the excited complex $(AD)^*$, resulting in the formation of an ion-pair A^-D^+ in the ground state. The parabola represent 2D-sections through the multidimensional potential curve as function of the normal coordinate q . The complex is considered as a super-molecule undergoing a radiationless transition from an excited $(AD)^*$ to a ground state (A^-D^+) . Two pathways of transition are considered starting from different initial vibrational states (I_1 and I_2) of the $(AD)^*$ (see text for explanation). The electron transfer indicated by the arrows show two fundamentally different types of transitions starting from initial state I_1 and I_2 . The undulated arrow shows the non-radiative transition from the highly excited vibrational state to the crossing P_c , while the thick arrow indicates the tunneling from the lowest vibrational state to the dissociated complex A^-D^+ . Images reproduced from [Merkel/Sackmann 2010].

A frequently posed question is whether quantum mechanics plays any role in biological processes. The electron transfer between electron donors and

acceptors embedded in proteins (such as between Cyt C and $(\text{BChl}^+)_2$ in Fig 4b) is an important example where tunnel processes can be important. The electron transfer between an excited complex $(\text{AD})^*$ of an electron donor (D) and acceptor (A) can be described in terms of the model of Figure 5b. The state of the dimers before and after charge separation is represented by a potential energy curve of a super-molecule in the two states $(\text{AD})^*$ and (A^-D^+) . The idea of describing such complexes as super-molecule was introduced by Theodor Förster in 1948 to calculate the resonance energy transfer (FRET) between excited energy donors and energy acceptors in ground state (see [Hopfield 1974]). After excitation of the complex into an excited vibrational state (I_1) it is deactivated radiationless until the crossing P_c is reached. There the rapid transition into the ground state A^-D^+ is most effective as predicted by the Franck-Condon principle. However, if we start from the lowest vibrational state I_2 the pathway depends on the temperature T . At high T the transition point P_c is reached rapidly by thermal excitation while at very low T the transition is still possible by electron tunneling, a genuine quantum effect. The rather slow transfer of electrons from the negatively charged Cyt C^- to the defect electron in the chlorophyll dimer is assumed to occur by tunneling. This follows from the experimental observation that rapid electron transfer occurs at low temperatures ($T > 10\text{K}$) and that the transfer rate is temperature independent. At high temperature an Arrhenius-like behavior of the electron transfer rate is observed as expected (see [Jortner 1980] or [Sackmann/Merkel 2010]).

Biology inspired water splitting systems: potential application as energy storing systems

Once we learned how elegant nature solved the problem of water splitting we can attempt to mimic the process and start building artificial energy storing facilities. Several attempts have been reported. That closest to biology is based on the use of electron acceptors mimicking the manganese complex (CaMn_4Ox) embedded in the manganese protein of the photosystem. The best choice of an artificial Mn-complex up to now is the cubic manganese complex cubane of structure Mn_4O_4 (see Figure 6a and [Brimblecombe 2008]). Due to its specific topology the complex can release oxygen by thermal excitation or photoexcitation and release of phosphinate. This unique property has been attributed to stretched Mn-O-bonds (see Figure XXa right side).

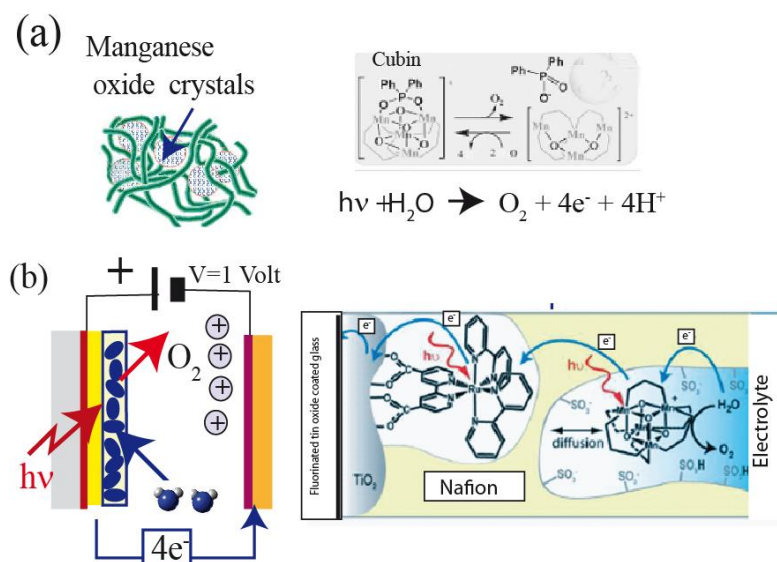


Figure 6.

Biomimetic water splitting system. (a) Left: doping of proton conducting Nafion membrane with cubane complexes. Right: Release of O_2 after thermal excitation or photo-dissociation of manganese complex. (b) The left side shows the electrolytic cell with stratified electrode. It consists of a glass plate covered by a fluorinated tin oxide (FT) electrode juxtaposed by porous TiO_2 with attached chromophore: a free ruthenium bipyridyl complex (RuBiPy [Park]) acting as photo-excitabile redox-system [Park 2010]. It mimics the function of chlorophyll. After excitation into the excited state it injects electrons into the anode generating a defect electron which can be refilled by electron transfer from the manganese complex.

The cubane core releases oxygen (O_2) with high yield upon removal of one **phosphinate** (see Figure 6a right side) either by photo-excitation in the gas phase or thermal excitation in the solid state. In order to catalyse the waters splitting and O_2 evolution the oxidized **cubane**, $[\text{Mn}_4\text{O}_4\text{L}_6]^+$, is dispersed in the proton conducting Nafion membrane which is deposited onto a conducting electrode (glass covered by fluorinated tin oxide shown in Figure 6b). To mimic the natural process of water splitting by sunlight the electrode is covered with porous TiO_2 doped with the chromophore RuBiPy . It acts as photosensitizer which injects electrons into the anode after excitation. The electron hole generated is replaced by electron transfer from the manganese complex. The reduced Mn-complex can be re-oxidized electrically via the cathode of the electrolyte cell by small voltages of 1 Volt.

In summary, the artificial manganese complex of the cubane family can mimic the function of the natural Mn-complex and oxidise water in artificial. Most interestingly, water oxidation (splitting) can be achieved both by electrical currents or by excitation of chromophores acting as redox-partner. The electrolyte cell could in principle be applied for energy storage by hydrogen generation. It is certainly an open question whether the principle can be applied on a large

scale which depends also on the synthesis of more potent and cheaper metal-complexes.

Another strategy of biomimetic water splitting was proposed by Weigele et al. [Weigele 2010]. In this case the electron donor is a zinc-porphyrin complex attached to bacteriophages by genetic engineering. The functionalized virus (acting as biological scaffolds) are embedded in a porous polymer matrix doped with iridium oxides. The metal oxide acts as an electron acceptor playing the role of manganese complexes in the photosynthetic system.

Swimming in the Sahara sand: Nature as material designer

Physicists or engineers who are involved in the design of new materials can learn much by studying living matter. Mother Nature developed a manifold of smart materials to optimize motional processes or to protect animals from external hazards. One stunning example is the sandfish of genus *Scincus*, a lizard which can dive deep into the desert sand and move with velocities of 0.1 m/sec (or 0.36 km/h), hence the name sandfish (see [Figure 9a](#)). Below sand, the animals move by exciting bending waves traveling from head to tail, while the feet most likely serve mainly the motion on the surface. This method of self-propulsion is remarkably similar to that of bacteria swimming in water or to snails crawling in grass as we will see below.

The motion of sandfish in the Sahara sand is determined by two physical concepts: the swimming of small objects at high friction (or high Reynolds numbers) and the reduction of solid friction by specific design of its skin. The sandfish skin is an impressive example of the evolution of smart surfaces that control the contact of living systems with the environment. Other examples of nature as surface designer (not considered here) are the control of wetting of leaves by water, mediated by adjusting the surfaces roughness (often called Lotus-effect [Herminghaus 2000]) and the generation of shells with outstanding mechanical properties by biomineralisation (reviewed by Ingrid Weiss [Weiss]).

Design and tribology of sandfish and snake skin.

The outer skin of reptiles (called Oberhäutchen) is covered by a thin layer of β -keratin forming beta pleated sheets such as silk. On the surface of snakes the β -keratin forms about 5 μm long and 100-nm thick hairs (microfibrilles) which lie

flat on the surface and point all with the ends towards the rear end (see Figure 7b, right side). The loose end point slightly upwards acting as barbes rendering the friction lower when the snakes move forward but higher if they move backwards or laterally. A very remarkable feature in the case of snakes is the small pores with 30-50 nm diameter which may serve the secretion of lubricant or the uptake of moisture.

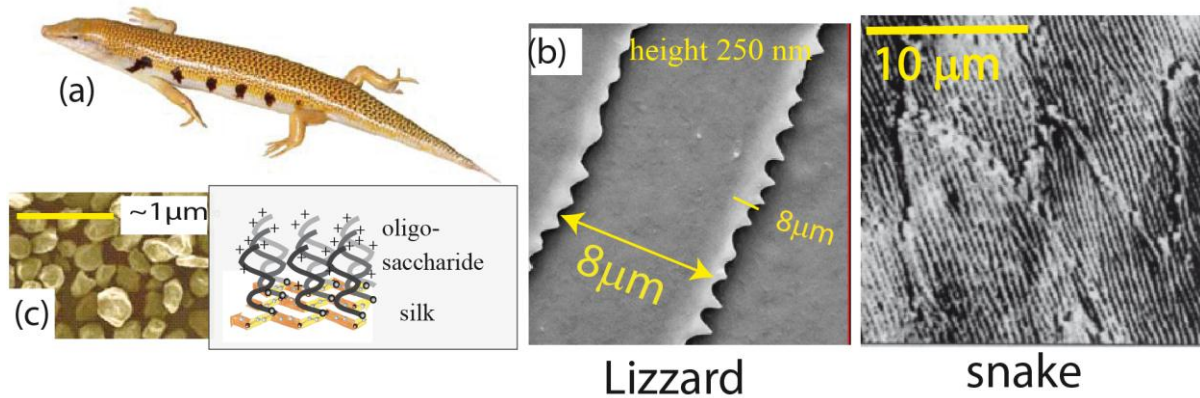


Figure 7. Some remarkable features of sandfish. (a) Image of sandfish *scincus albifasciatus*.

(b) Left: Surface profile of skin (Oberhäutchen) of lizard (*scincus albifasciatus*) exposing comb like protrusions on the back but not the belly. Right: Surface profile of snake skin which is made up of parallel β -keratin bundles (silk hairs) with the tips pointing to the back.

(c) Left: particles of desert sand. Right: schematic view of oligosugar-filaments coupled to plate of β -keratin to which oligosaccharide chains are coupled. The hairs are assumed to be charged during motion due to frictional electricity.

The surface of the sandfish exhibits several remarkable and unique features [Baumgartner 2007]:

- The keratins contain a high amount of sulphur which is assumed to be responsible for the high elastic constant of the Oberhäutchen, but it does not contain hard inorganic material, such as silicates or lime as assumed occasionally [Baumgartner 2007].
- A unique feature of the β -keratin of sandfishes is the exposure of neutral oligosaccharide chains. Mainly of the neutral sugar groups are coupled to serine side chains of the β -keratin but which can also be phosphorylated
- Most remarkable is the repulsive force exerted by the skin on AFM tips composed of silicon-nitride with or without silicon oxide layers. This repulsion is the same on the back and the belly, showing that it is not due to some specific surface profile, such as the comb-like protrusions at the back. However, removal of the sugar side chains by enzymes results in strong stickiness, showing that the repulsion is mediated by the surface chemistry and most likely due to polymer

induced forces (see below).

- An important property, closely related to the glycosylation of the keratin layer, is the astonishing resistance to abrasion which can be tested by treatment with sandblaster. Comparison with different metals revealed an astonishing strong resistance to abrasion. While steel showed remarkable abrasion after 10 hours of sandblasting the skin showed no remarkable effect after such a treatment [Rechenberg 2009].

Friction control by polymer brushes

The control of adhesion and friction between solids by polymer films is an intensively studied field of biomimetic research []. Nature made full use of this trick at all levels of organization. Without constant lubrication of the gap between moving joints of our body we cannot move, as people with Arthritis know well. Our knee joints are typically subjected to pressures of 5 MPa. In joints, the friction is reduced by the glycoprotein lubricin (see [Lubricate Joints 2007]). These ~230 kDa macromolecules with contour length $L_c \approx 200$ nm are coupled to collagen covered surfaces. The analogy with the structure of the sandfish skin shows first, that the concept was invented by nature long before the advent of mammals and second, that nature uses a successful concept again and again.

The composition of the oligosaccharides of sandfish is not known yet, but their effect on friction has been well studied. For this purpose the skin is fixed on a glass plate tilted with respect to the horizontal by an angle α . Then a layer sand is deposited on the surface. By measuring the maximum angle above which the sand starts to slide one obtains the frictional coefficient μ_f , which is defined as the ratio of the frictional force F_p parallel to and the normal force F_n perpendicular to the plate (see [Rechenberg]):

$$\mu_f = \frac{K_r}{K^n} = \tan \alpha_c$$

The critical angle is 21° for sandfish skin, 29° for glass and 36° for teflon. Surprisingly the friction is the same at the back and belly of the sandfish despite of the lack of the comb structure on the latter [Baumgartner 2007]. A possible function of the comb-shaped protrusions on the back is to minimize the contact area with sand corns at the back in order to compensate for the gravity. Consider a lizard swimming 10 cm below the surface. The pressure exerted on the back is $p \approx 1600$ Pa for a specific weight of 1.6 g cm^{-3} which would correspond to a strong frictional force. The sand particle exhibits diameter of about 0.5 mm and thus covers about 10 combs which would reduce the friction drastically, provided the polymer film is stable enough.

Polymer-induced repulsion forces:

The interaction of the skin covered by polymer brushes and sand particles can be described by the Donnan-Edwards potential which accounts for the interaction of

two surfaces separated by polymer brushes, provided the separation between polymers is slightly smaller than the radius of gyration R_g .

$$V_{rep}(h, R_g) \approx k_B T \rho_0 \left(\frac{R_g}{h} \right)^2 \exp \left[-\frac{3}{2} \left(\frac{h}{R_g} \right)^2 \right] \quad ()$$

Here ρ is the lateral density of the polymer chains. This equation holds below or near the overlap concentration $\rho_0 R_g \leq 1$. The disjoining pressure is of the order of $p_{disj} \approx V_{rep}(h, R_g)/h$. To gain some insight into the strength of the disjoining pressure we consider an oligosaccharide chain with $R_g \approx 10\text{nm}$ and assume $\rho_0 \approx R_g^{-1}$. For $h \approx R_g$ the repulsive pressure is $p_{disj} \approx 2\text{kPa}$. This value is about equal to the pressure exerted on the back if the lizard swims 10 cm below the surface.

Friction electricity may help the repulsion by hair raising effect.

Under the conditions of low humidity of the desert the friction between sand and the skin of the lizard results in high electric charging of the silk like surface [Rechenberg 2009]. It has been speculated that the magnetic field generated by the moving animal might generate a repulsive force and reduce friction. However, the force would be too weak to lift sand particles from the surface against gravity. A more likely effect of the charging could be the stretching of the oligosaccharide filaments coupled to the keratin filaments. It is well known that the persistence length of polyelectrolytes is much larger than that of neutral macromolecules. In air the stretching effect would be larger since the charges are not screened by water molecules.

Self-propelled swimming at very low Reynolds numbers: G. Taylors Theory

There are close analogies between the swimming of bacteria and sandfish although the properties of water and granular media are very different. To show this analogy we first address the question: why bacteria cannot swim like fish or humans in water by moving their appendages? The reason is that nature had to account for the scaling laws of physics. Fish swim by generating hydrodynamic flow fields moving towards their back side. The well-known laws of hydrodynamics of viscous fluids teach us that the flow velocity is zero at the surface resulting in a velocity gradient $\partial v / \partial z$ perpendicular to the surface (defined as z-axis) which generate a Newton frictional force

$$F_f = \eta \frac{dv}{dz} \quad (1)$$

where η is the viscosity of the fluid. To fulfill the condition of force equilibrium at the surface (Newton's third law) the frictional generates the momentum for the advancement of the body. In inhomogeneous flow fields the molecules are also subjected to inertial forces f_i (per unit volume) since they change their

velocity vector while moving in the direction of the gradient: $F_i = \rho \vec{v} \text{ grad } \vec{v}$, where ρ is the mass density. Taken together these consideration show that swimming is determined by the interplay of frictional and inertia forces. The swimming behavior of animals is therefore determined by the dimensionless Reynolds Re which is equal to the ratio of the accelerating force to the frictional force:

$$Re = \frac{\rho v^2 L^2}{\eta L v} \quad (2)$$

Dimensionless numbers such as Re play key role for the design of ships and airplanes since it shows the engineer how the behavior of his design depends on the size L and the density ρ of the medium. In particular he knows that a large ship swimming in water behaves as a small model swimming in mercury. There are many examples showing that natural evolution was guided by scaling laws (as was first recognized by Galilei). The change of the swimming behavior of fish and bacteria is such an example. For a typical fish ($L \sim 1\text{m}$, $v \sim 10\text{m/sec}$) $Re \sim 10^4$ and the energy dissipated is very small. For a cylindrical fish of

circumference B the force is of the order $F_r = -\eta \frac{dv}{dz} B L$. For bacteria ($L \sim 1\mu\text{m}$,

$v \sim 10\mu\text{m/sec}$) the Reynolds number is of the order of $Re \sim 10^{-6}$. Therefore nearly all energy generated by the motor is dissipated into heat. In summary, bacteria moving in water feel like a fish swimming in honey [Taylor 1952].

There was another problem nature had to solve by using flagella as agitator of motion. Long cylinders behave very different from spheres. The laminar flow field decays very slowly with distance: $v \propto r^{-1}$ and a moving cylinder has to carry much more fluid than a sphere (see [Landau § 20]). Fortunately these problems are less severe for rapidly oscillating long objects as was first recognized by the most prominent 21th century expert in hydrodynamics G. Taylor [Taylor 1952]. In a celebrated paper he showed that small animals with flagella can swim if they generate traveling undulation waves running from the head to the tail (such as rope waves), thus generating a force directed opposite to the direction of the wave. For cylindrical objects of radius a the velocity is given by

$$v = \frac{1}{2} A^2 q^2 \frac{K_0(qa) - 1/2}{K_0(qa) + 1/2} U \quad (3)$$

q is the wave vector $q = \frac{2\pi}{\lambda} = \frac{2\pi v}{U}$, K_0 is the Bessel function of first kind and U

the phase velocity. Please note that this equation holds not only for unicellular organisms or sperm which excite planar oscillations but also for the *E. coli* bacteria rotating their helical shaped flagella, since the rotating wave can be decomposed into two perpendicularly oriented planar waves phase shifted by $\pi/2$. The most important result is that the velocity is a quadratic function of the undulation amplitude and the frequency, that is the self-propelling of bacteria is an effect of second order. Taylor designed macroscopic artificial

animals with rotating motors to verify his theory. He showed in these experiments that the swimming technique of bacteria works only at high Reynolds numbers. Therefore large animals could use this technique only for swimming in high viscosity media but not in water and nature had to invent a new swimming technique for the evolution of fish.

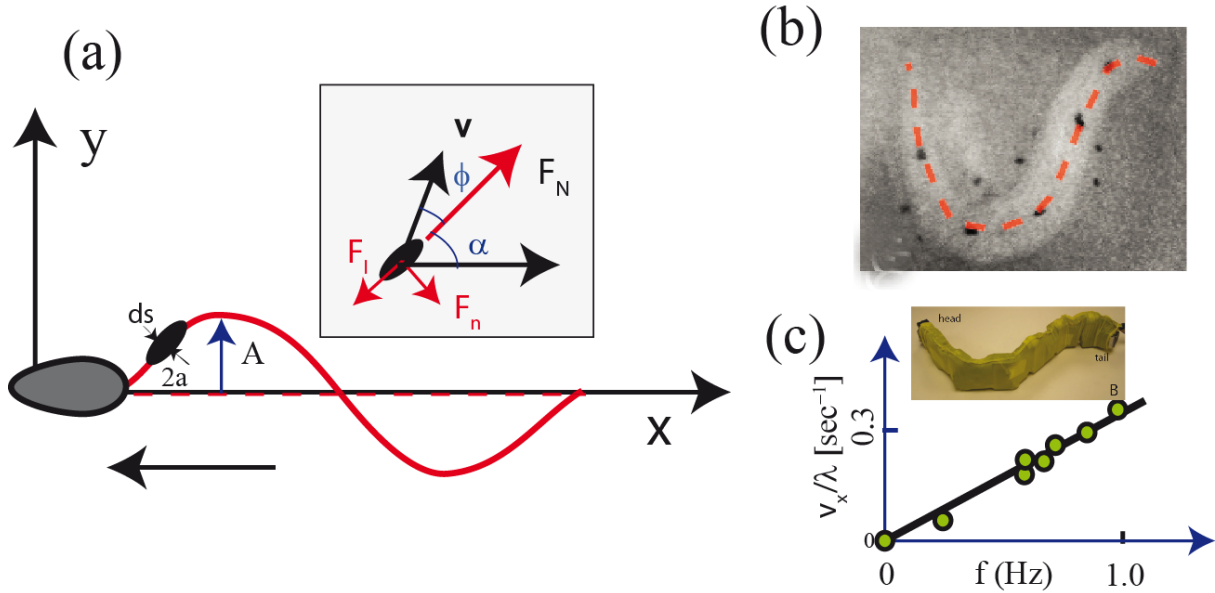


Figure 8: (a) Definition of forces on local segment of flagella or snake like animals (water snake or sperm cells) moving by agitating of travelling waves of amplitude A and angular frequency ω along the elongated body from head to tail. v is the local velocity of the segment, F_p and F_n are the forces parallel and perpendicular to the local segment and (b) snapshot of sand fish moving below sand visualized by X-ray imaging (taken from [Maladen 2011]). (c) Measurement of normalized velocity of model sandfish (see inset) as function of frequency of excitation.

The analogy between the swimming of sandfish and bacteria becomes evident if we have a closer look at the physical basis of the propulsive force (see Figure 8). We consider the frictional force on a flagella segment of length δl moving with momentary velocity v . The frictional force on the element is $\delta F = \zeta_n v_n + \zeta_p v_p$ where v_n and v_p are the velocities and ζ_p and ζ_n the frictional coefficients in the tangential and normal direction [Gray Hancock 1955]. The key point is the anisotropy of the frictional forces. In liquids the frictional force in the tangential direction is $\zeta_n \approx 2\pi\eta L/k_B T \ln L/a$ and is by a factor of 2 smaller than in the normal direction: $\zeta_p/\zeta_n = 2$. A closer inspection of Figure 8 shows that the resulting frictional force on an element δl moving with an oblique angle θ with respect to the body axis is

$$F_{res} \approx \zeta_p v_p \cos \vartheta. \quad (4)$$

According to Newton's third law F_{res} is a measure for the propulsion force. It is determined by the anisotropic friction exerted by the moving fluid on the flagella. As pointed out already by Taylor, the bacteria and sperm swim in fluids as screws that are driven into the wall by rotating with a screw driver.

Let us now consider the situation for sandfish. Similar to flagella of sperm or snakes, it generates propulsion forces by agitating travelling bending waves moving along its slender body. As in the case of bacteria the driving force is determined by the direct frictional coupling of the sand particles with the skin. The major difference is that the sand is a viscoelastic medium and the motion is also controlled by the deformation of the sand by the moving animal [Maladen 2011]. Following a theory by Herrmann et al [Herrmann 1993] the forces on a small surface element of the body moving in sand can be expressed as

$$F_n = k\delta^{3/2} - G'' v_n \delta^{1/2} \quad (5a) \quad \text{and} \quad F_{fp} = \mu F_n \quad (5b)$$

The right term of Equation (5a) accounts for the elastic deformation of sand and is expressed in terms of the Hertz model of deformation of elastic body by a small objects. Therefore, k is an effective elastic constant and δ the indentation induced by the normal force. The right term accounts for the energy dissipation by friction, where G'' is the effective loss modulus of the sand and v_n is the normal velocity. Equation (5b) is the classical Coulomb equation of the effective frictional force in the tangential direction.

Similar to Taylor a group of engineers at the Georgia Tech designed robots which can mimic the motion of sandfish (see [Maladem 2011]). The robots are composed of arrays of small cylinders which can rotate about an axis perpendicular to the plane of undulation. By periodically rotating (see Figure 10c) the segments by small angles the robots can mimic the locomotion of snakes. In a separate experimental study by Ding et al. it was shown that one can calculate the frictional force on a long cylinder moving in sand by dividing its surface into small plates and integrate over the forces on all of these elements. The pertinent results of these studies are [Ding 2011]:

- The locomotion of snakes or sandfish on the surface or within sand is determined by the anisotropic frictional force on the surface, in analogy to the swimming in fluids at very small Reynolds numbers.
- The swimming velocity is a linear function of the undulation frequency. This contrasts with the swimming of slender objects in water where the velocity depends on the square of the amplitude and frequency.
- The mechanism of force generation in sand is different from that applied

by worm like animals (snakes, lizzards or nematodes) to move on granular surfaces. In the latter case forward thrust is generated by the resistive forces arising by pushing the body sideward

The role of the feet of sandfishes is still debated. The X-ray observations suggest that the feet lie close to the body and play a minor role. An argument in favour of this conclusion is the good agreement between the calculated and the observed motions of the sandfish robot [Malade 2011]. On the other side Baumgartner et al provided evidence that the feet perform “paddling-like movements” and in this way enforce the thrust [Baumgart 2009].

Why is it interesting to study the motion of worm-like animals in granular media or soft surfaces, besides our desire to understand the role of physics during biological evolution? One technical motivation is the design of robots which can move in sand, quicksand or mud. A medical reason is the understanding of the motion of worm-like parasites in our body. Intestinal parasites (such as hookworms) cause some of the most common world-wide infections.

II. Nature as engineer and material designer.

On the way to moving animals Taylor: self-propelling in viscous fluid

Numerous observations suggest that evolution of new species took place by slight modification or refinement of existing materials or concepts. A beautiful example is the advent of mobile bacteria through the attachment of flagella to proton driven rotating motors. We will see how nature controls motion by making use of solid state phase transitions, a concept developed by metallurgists to generate hard steel.

The survival of bacteria under harsh conditions required a smart search strategy to find nutrition or to escape live damaging conditions. Figure 8 shows that motion of E. coli bacteria consists of repeating sequences of straight swimming followed by random motions [Berg 2003]. The rapid switching between the two states of motion is triggered by a sudden shape change of the flagella. During the directed swimming the filaments are slightly undulated and rotate collectively while they form super- helices and rotate independently to move randomly. The switching occurs within 0.1 sec. How can this be? To solve the problem nature invented the concept of martensitic solid-solid transitions described below.

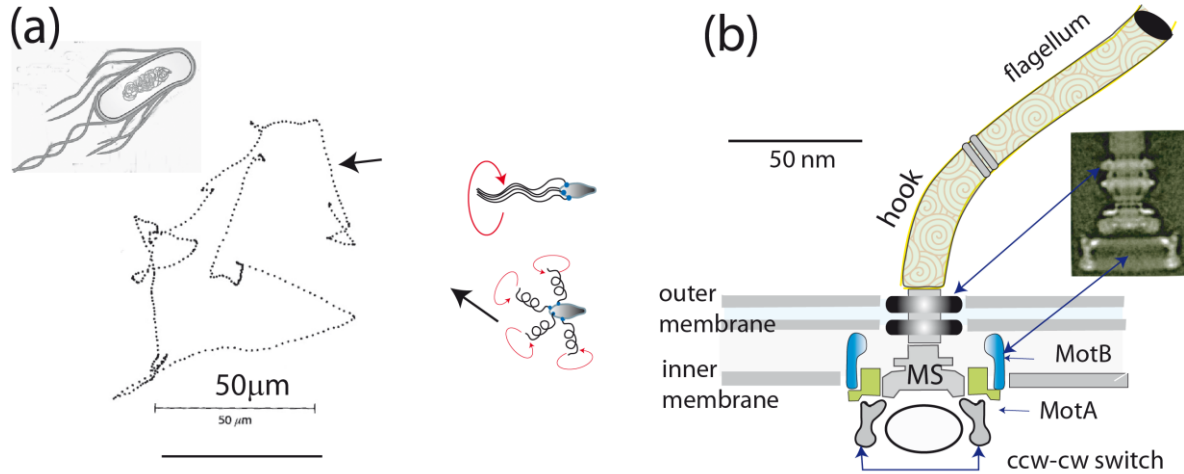


Figure 9:

(a) Left: typical motion of bacteria consisting of nearly straight trajectories and local tumbling motion serving the random changes of new direction. The ratio of the times in the straight and random motion is $r_t=0.1$. Right side: correlation between direction of motion and the shape of flagella which differ by the pitch of the superhelical shape. Please note that they move synchronously if they rotate in the counter clock wise direction (ccw) but fan-out during clockwise (cw) rotation. At physiological temperatures the flagella rotate for one second cc and for a tenth of a second in ccw direction. The switching is mediated by a change of the flagella shape described in Figure 10.

(b) Schematic view of rotating motor of *E. coli* bacteria. In analogy to technical motors, it consists of a rotor (the protein ring MS) which is embedded in the cell plasma membrane and a stator fixed in the cell wall which serves as a slide bearing in which the shaft of the flagellum rotates. Details see review by H. Berg [Berg 2003] and [Sackmann/Merkel 2010]. The right inset shows an electron micrograph of the motor. (Modified after N. Fransis et al. *J Mol. Biol* 235:1261, 1994))

On the energetics and mechanics of force generation of rotating motors. The rotating motors are activated by proton fluxes through the cell envelope from the periplasm to the cytoplasm as shown in Figure 6b. Some species such as **Leuchtbakterien** in the ocean) move by potassium driven rotating motors which rotate with 1700 Hz.

The energetics of rotating motors. The driving force is determined by the electrochemical potential difference $\Delta\mu_{elch}$ between the extracellular space (“out”) and the cytoplasm (“in”):

$$\Delta\mu_{elch} = k_B T \ln \left\{ \frac{[H^+]_{out}}{[H^+]_{in}} \right\} + e\Delta\psi \quad (1)$$

$\Delta\psi$, $[H^+]_{out}$ and $[H^+]_{in}$ are the electrical potential difference (\sim in mV), and the proton concentrations. Typical values are: $e\Delta\psi = -120\text{meV}$ $[H^+]_{out} = 2 \times 10^{-8}$ M and $[H^+]_{in} = 10^{-6}$. At 25°C the contribution by the pH-gradient is +50 mV and of the electrical -120 mV. A surprising result is that the electrical potential contributes substantially to the driving force. Therefore the bacteria can even swim if the proton gradient is zero.

Estimation of torque of ATP-Synthase Motor

The torque generated by the motor has been measured by the elegant technique shown in the Appendix (see Figure A.3), yielding $M_{act} = 3 \cdot 10^{-18}$ Nm. By application of the model discussed above (see Figure YYY) we can estimate the torque as follows: If the COO^- -group of the aspartic acid is protonated and pulled into the hydrophobic domain it gains the Born energy w_B of an O^- ion. If we treat the bilayer as a non-conducting slab of dielectric constant $\epsilon_M \approx 2.5$ embedded in water ($\epsilon_w \approx 80$) we obtain

$$\Delta F_{Born} \approx \frac{z^2 e^2}{8\pi\epsilon_0 R} \left(\frac{1}{\epsilon_M} - \frac{1}{\epsilon_w} \right) \quad (2)$$

With $\epsilon_0 \approx 8.85 \times 10^{-12} \frac{\text{Assec}}{\text{Vm}}$; $e = 1.6 \times 10^{-19} \text{Assec}$ and the oxygen ion radius of 0.74 nm one obtains $\Delta F_{Born} \approx 30 k_B T$. Since the step width is equal to the diameter of lipid molecules ($d \approx 1\text{nm}$) the pulling force is $f \approx 10^{-10}$ N. The torque exerted by this force is $\vec{M} = \vec{f} \times \vec{R}$. With a radius of the rotor of 25 nm (see [Berg 2003]) ($2.5 \cdot 10^{-18}$) in good agreement with the measurement.

Subsecond switching of rotation direction by solid-solid phase transition

A stunning and enigmatic capacity of the rotating motor is the fast change in rotating direction by changing the shape of the 4 μm long flagella. Even more surprising is the rapidity of the transition occurring within ≈ 60 msec [Berg 2003]. Elegant studies of a Japanese groups (see [Kamiya 1979]) showed that the rapid shape change is a non-diffusive solid-solid transition of the flagella wall which is very similar to the martensitic transition of metals used to harden steel (see Appendix 3). This beautiful example shows that nature makes use of solid state transitions in order to optimize biological processes. The flagella (length 4 μm diameter 20nm) consist of a single 50 kDa protein flagellin. Electron microscopy studies of natural and artificial flagella (generated by self-assembly of flagellin in solutions) show that the wall of the tube consists of two-dimensional crystals which are formed by parallel arrangements of 11 filaments (protofilaments) of flagellin. The 2D-crystal can exist in two modifications called R- and L-form. In the R-state the protofilaments are tilted

with respect to long axis AA' by $\phi = +7^\circ$ and in the L-state by $\theta = -2,5^\circ$ (see Figure 9). Tubes consisting of a single conformation (R or L) would be straight and the protofilaments would form right or left handed helices. The vertical distance of the protomers is $\Delta z = 0.08nm$ shorter in the R-form than in the L-form

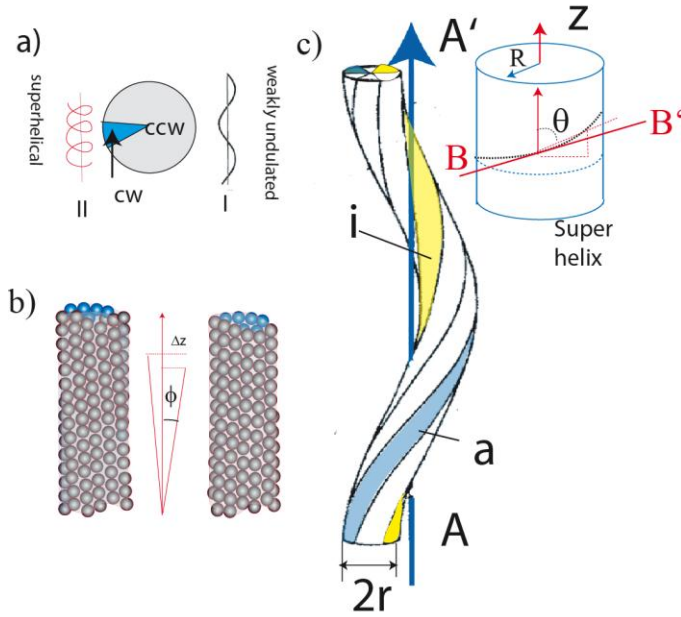


Figure 9.

Shape transformation of flagella as martensite-like transition (see also figure A3 of Appendix A). (a) Two major shapes of flagella and times of clockwise (ccw) and counterclockwise (ccw) rotation and clockwise (cw)-direction. In the undulated shape (state I) the flagella rotate synchronous in the counter direction while they fan out and rotate uncoordinated in the superhelical shape (state II). (b) The flagelline protofilaments forming the tube wall are tilted and form a helix, with the long axis being tilted to the right (R-state, tilt angle $\phi = +0.8^\circ$) or to the left (L-state, tilt angle $\phi = -0.25^\circ$). Note that the pitch of the helix is shorter in the R-state.

(c) Hypothetical structure of superhelix with Radius R which is composed of only 6 proto-filaments to simplify the discussion of the superdrilling in the text. The parameters characterizing the superhelix are shown in the inset (top right). Please distinguish between global (AA') and local axis (BB'). The latter form an angle θ with respect to AA' and is called **the twisting angle**. A closer inspection of figure shows that $\cos \theta = \frac{dz}{ds} = \frac{P}{2\pi\sqrt{(R^2 + p^2)}}$, where $P = 2\pi p$ is the pitch of the

helix, while the denominator is equal to the filament contour length S per pitch (see Eq. (1)).

The switching of the flagella ability between the undulated (I) and superhelical shapes (II) is mediated by the transition of a fraction of the filaments from the longer L into the shorter R-form. This decay of the 2D crystal into coexisting R- and L-forms can be described in term of shear- induced twin formation as shown in Appendix 3 (see also [Kamiya]). In the case of tube formation the high elastic energy costs associated with the mismatch between the two lattices can be relaxed by the formation of a superhelix. In this case the shorter filaments (contour length S_2) run along the inner and the longer (length S_1) along the outer seam of the superhelix (see Figure 9c). The major reason for the super-twisting is the specific topological properties of helices: both the local curvature ρ^{-1} and the contour length S depends only on the pitch ($P=2\pi p$) und the radius (R) (see Figure 9)

$$\rho^{-1} = \frac{R}{R^2 + P^2} \quad S = 2\pi\sqrt{(R^2 + p^2)} \quad (3)$$

With some effort one can show that for topological reasons only a limited number of superhelices can be generated. To see this we start from the pure L-state forming a tube of radius R . For a given value of the length difference between the $\Delta S = S_1 - S_2$ there is only one Radius R for which the number of monomers per pitch length for each proto-filament is the same. Be $\Delta s = \frac{S_1 - S_2}{S_1 + S_2}$ the normalized difference of contour lengths. With the help of Eq. (3) one can show that the radius of the superhelix is determined by

$$\Delta s = \frac{2r R}{R^2 + p^2} \quad (4)$$

A further condition must be fulfilled by the difference $\Delta\theta$ of the local twisting angles at the outer and inner side of the superhelix:

$$\Delta\theta = \frac{r p}{R^2 + p^2} \quad (5)$$

Note that in both cases the denominator is equal to S^2 . This condition is easily verified by considering the local slope of the helix with respect to the long axis. Optimal molecular packing in the crystal lattice requires that ΔS is equal to multiples of the lattice constant Δz : $\Delta S = n \Delta z / S$. By analyzing many electron microscopic images of natural filaments and tubes formed by self-assembly of the filaments the above model was verified. In particular it was shown that the slightly undulated (I) and the superhelical state (II) form if 2 and 4 protofilaments are changed from the L into the R-form. These states exhibit the lowest elastic energy [Asakura], [Kamiya], [Calladin].

References water splitting

[Brimblecombe2008] Brimblecombe, G., et al. (2008) Sustained water oxidation photocatalysis by a bioinspired manganese. *Angew. Chem. Int. Ed.* 47: 7335-

[Dismukes 2009] Dismukes et al. (2009) *Acc. Chem Res.* 42(12): 1935-1943.
Service (2009) *Science*, 325: 1200-1201.

[Park Y.2010] Park, Y., et al. (2010) Organic dye-sensitized TiO₂ for the redox conversion of water pollutants under visible light. *Chem. Commun.* **46** : 2477-9

[Hopfield 1974] Hopfield, J.J. (1974) Thermally Activated Tunneling. *Proc. Nat. Acad. Sci. USA* **71**: 3640-3644,

[Sung 2010] Yoon Sung Nam et al. (2010) Biologically templated photocatalytic nanostructures for sustained light-driven water oxidation. *Nature Nanotech.* 5: 340-344

[Kamiya] R. Kamiya, et al (1979) Transition of bacterial flagella from helical to straight forms with different subunit arrangements. *Journal of Molecular Biology* 131:725-742.

[Miller 1953] S. L. Miller (1953): A production of amino acids under possible primitive earth conditions. In: *Science* **117**: 528–529.

[Gutknecht 1987] J. Gutknecht (1987) Proton/hydroxide conductance and permeability through phospholipid bilayer membranes. *PNAS* 84: 6443-6446.

[Deamer1987] Deamer DW. (1987) Proton permeation of lipid bilayers. *J. Bioenerg Biomembr.* 19:457-79.

[Dietz 2004] M. Dietz et al Proton-powered subunit rotation in single membrane bound FoF₁ ATP synthase. *Nature Struct. Mol. Biol.* 11 135-13x (2004).

[Rondeles 2005] Y. Rondelez et al. [2005) Highly coupled ATP-Synthesis by F₁-ATPase single molecules *Nature* 433: 773-777 (2005).

[Gräber] P. Gräber Kinetics of proton-transport coupled ATP-synthesis in Chloroplasts in *Bioelectrochemistry III.* (G. Milazzo and .Blank eds.). Plenum Press 1990

[Renger 2007] Renger, G., and Kühn, P. (2007) Reaction pattern and mechanism of light induced oxidative water splitting in photosynthesis. *Biochim. Biophys. Acta* **1767**: 458-471]

[Jortner 1980] Jortner, J., (1980) Dynamics of electron transfer in bacterial photosynthesis *Biochim. Biophys. Acta* 594 193-230 (1980)

[Deisenhofer]

[Zinth 2005] Zinth, W., Wachtveitl, J. (2005) The first picoseconds in bacterial photosynthesis – ultrafast electron transfer for the efficient conversion of light energy” ChemPhysChem, 6, 871 – 880 (2005).

[Berg Stryer 2003] J.Berg, J.Tymoczky and L.Stryer Biochemie Spektrum Verlag Heidelberg 2003

[Pasek 2008] Pasek, MA., (2008) Production of potentially biotic condensed phosphate by phosphorus redoxchemistry. Angew Chemie Int. Ed. **47**: 7918-7920

References:

Nature as surface designer

[Lubricate Joints 2007] Jay G. et al. (2007) Association between friction and wear in diarthrodial joints lacking lubricin Arthritis Rheum. 56: 3662–3669.

[Baumgartner 2007] Baumgartner, W. et al. (2007) The Sandfish’s Skin: Morphology, Chemistry and Reconstruction. Journal of Bionic Engineering 4: 1-9.

[Rechenberg 2009] Rechenberg, I., et al. (2009) Schlussbericht BMBF projekt F- 0311967A

[Herminghaus]

[Bruinsma 2000] Bruinsma, R., et al . (2000)Adhesive switching of membranes: Experiment and theory. Phys Rev E. 61: 4253-4267

[Weiss] Weiss, J., Jewels in the Pearl ChemBiolChemI. 297 – 300

[Hazel 1999] Hazel, J., et al. (1999) Nanodesign of snake skin for reptation locomotions via frictional anisotropy. J of Biomechanics **32**: 477.484

[Dolan-Edwards 2010] P.-G. deGennes, Scaling Concepts in Polymer Physics Cornell University Press, Ithaca, NY, 1979. .P. Born et al (2010) J. Phys. and Chem. Solids 71, 95-99

[Baumgartner 2007] Baumgartner (2007) Journal of Bionic Engineering 4: 1-9

[Jay 2007] Jay, G. (2007) The role of lubricin in the mechanical PNAS 104: 6194–6199

[Raviv] Raviv, U., et al. Lubrication by charged polymers Lubrication by charged polymers. Nature 425: 163-165

References sandfish:

[Blake 1972] Blake, JR. (1972) A model for the micro-structure in ciliated organisms Journal of Fluid Mechanics 55: 1-023

[Gray Hancock 1955] J. Gray, G. J. Hancock (1955) The propulsion of sea-urchin spermatozoa. J. Experimental Biology **32**: 808-814

[Baumgart 2009] Baumgart, W., et al. (2009) Investigating the Locomotion of the Sandfish in Desert Sand Using NMR-Imaging. PLoS ONE Vol. 3.

[Maladen 2011] Maladen, RD. et al (2011) Undulatory swimming in sand: experimental and simulation studies of a robotic sandfish. *Internat. J. Robotics Research* 30: 793-804

[Herrman 1993] Lee J and Herrmann H (1993) Angle of repose and angle of marginal stability: molecular dynamics of granular particles. *J. of Physics A* 26: 373–383.

[Ding 2011] Ding, Y., et al. (2011) Drag induced lift in granular media. *Phys Ref letter* 106:028001 -4

[Gray 1964] Gray, J., Lissmann, HW. (1964) The locomotion of nematodes *J. Exp. Biol.* (1964), **41**: 13S-154

References Rot Mot.

[Berg 2003] H. C. Berg. The rotary motor of bacterial flagella (2003) *Annual Review of Biophysics* **72**: 19-54

[Asakura] S. Asakura, and T. Iino (1972) Polymorphism of Salmonella flagella as investigated by means of in vitro copolymerization of flagellins derived from various strains. *J. Mol. Biol.* **64**: 251-256

[Kamiya 1979] R. Kamiya, et al (1979) Transition of bacterial flagella from helical to straight forms with different subunit arrangements. *J. Mol. Biol.* **131**: 725-742.

[Calladin 1976] C. R. Calladine (1976) Design requirements for the construction of bacterial flagella *J. Theor. Biol.* 57:469-489

Appendix A: Proton gradient generation by cold splitting of oxygen in mitochondria F0/F1-ATPase.

In mitochondria of eukaryotes the electrons stored in the energy-rich and H-sequestering molecule NADP^+ , serve the cold-splitting of oxygen into water in the dark. The NADPH is generated by various metabolic processes including glycolysis. As illustrated in Figure A1 the electrons are transferred from NADPH over three electron storage-and-release proteins (the Redox-system I-III in Figure A1a) which are embedded in the inner membrane of mitochondria. Oxygen splitting occurs at the protein complex III (the so called Cytochrome c Oxidase). At each step marked by double arrow in Figure A1a enough energy is gained (in the form of pH-changes) to synthesize one ATP by the ATP-synthase requiring $30 k_B T$. Figure A1c shows the analogy of irreversible electron separation at pn-transitions of semiconductures.

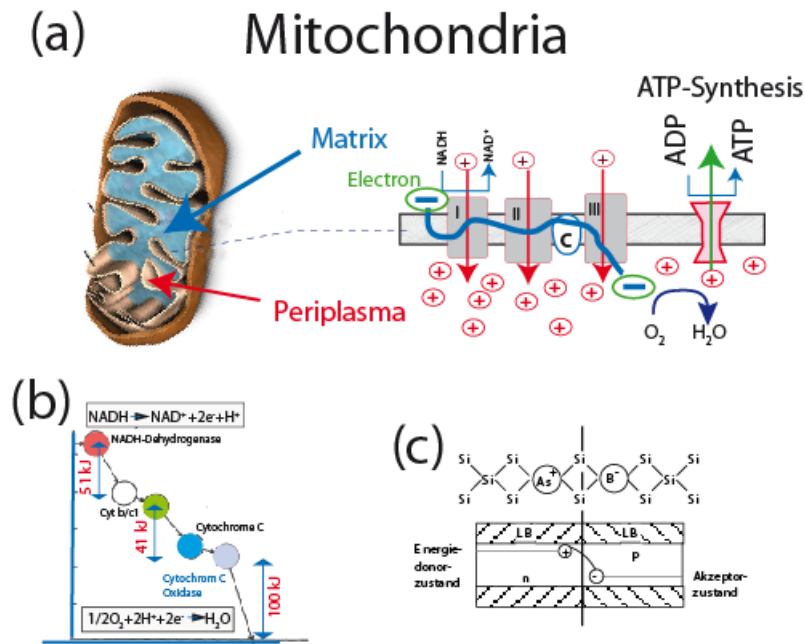


Figure A1

Transformation of photon energy in protomotoric force by photosystem of purple bacteria through the cyclic electron transfer across membrane of photosystem. Electrons are generated by photodissociation of the bacteriochlorophyll dimer ($B\text{-Chl}_2$). They flow over several redox partners (a chlorophyll monomer, pheophytin and two quinones (see Glossar)) to the electron acceptor Cytochrome C (Cyt C) as shown by the red arrow. The electron flow is associated with a proton flux generating the proton motoric force. The electron cache Cyt C can store several electrons and deliver them to the electron hole generated in $B\text{-Chl}_2$.

Single electron transfer by Quinones: Quinones belong to the few organic molecules which can form stable free radicals. They can thus serve the successive transfer of single electrons and fulfill the rules of stoichiometry. By coupling the benzene ring to hydrophobic chains the molecules can transport single electrons in Membranes. The following scheme shows the examples of **Plastoquinon** (length of hydrophobic chain $n = 9$) and **Ubichinon** ($n = 6-10$).

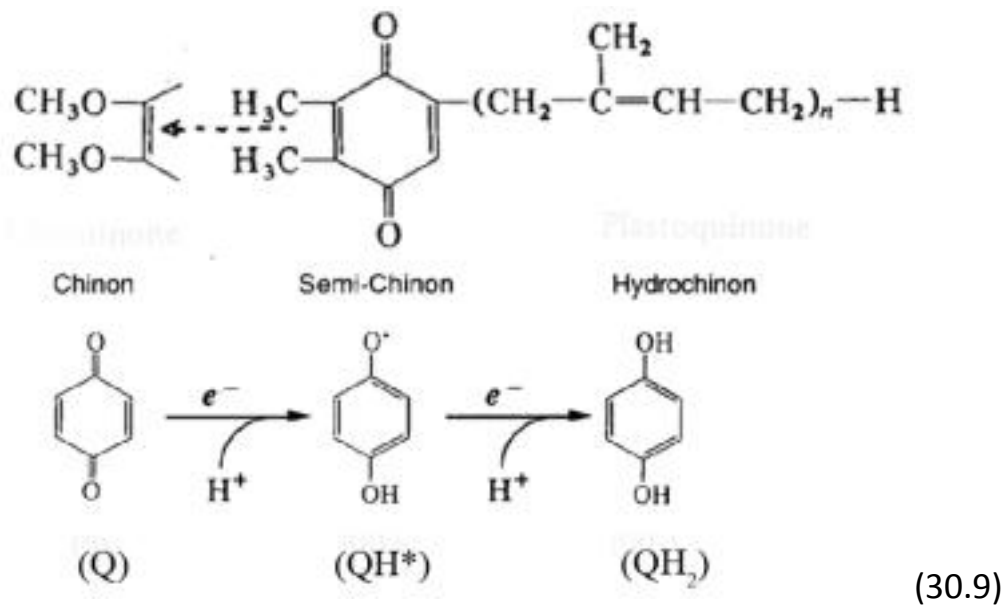


Figure A1: Storage of one electron on quinone forms the stable free radical semi-quinone which is transformed to hydroquinone after transfer of a second electron.

Appendix B The reversible ATP synthase couples the universal protomotoric force to biochemistry.

The evolution of bioenergetics until the advent of oxygen producing photosynthesis (about 2.4×10^9 years ago) culminated in the development of the ATP synthase and rotating motors enabling bacteria to search for nutrition (see Figure 6). From the point of view of physics of nano-machines the ATP synthase is absolutely fascinating since here nature managed to couple the biochemical generation of biological energy to a universal physical force: the pH-gradient. This revolutionary principle was first recognized 1960 by P. Mitchell, who postulated the chemo-osmotic hypothesis in 1960. But it took more than 20 years before biochemists fully accepted this idea.

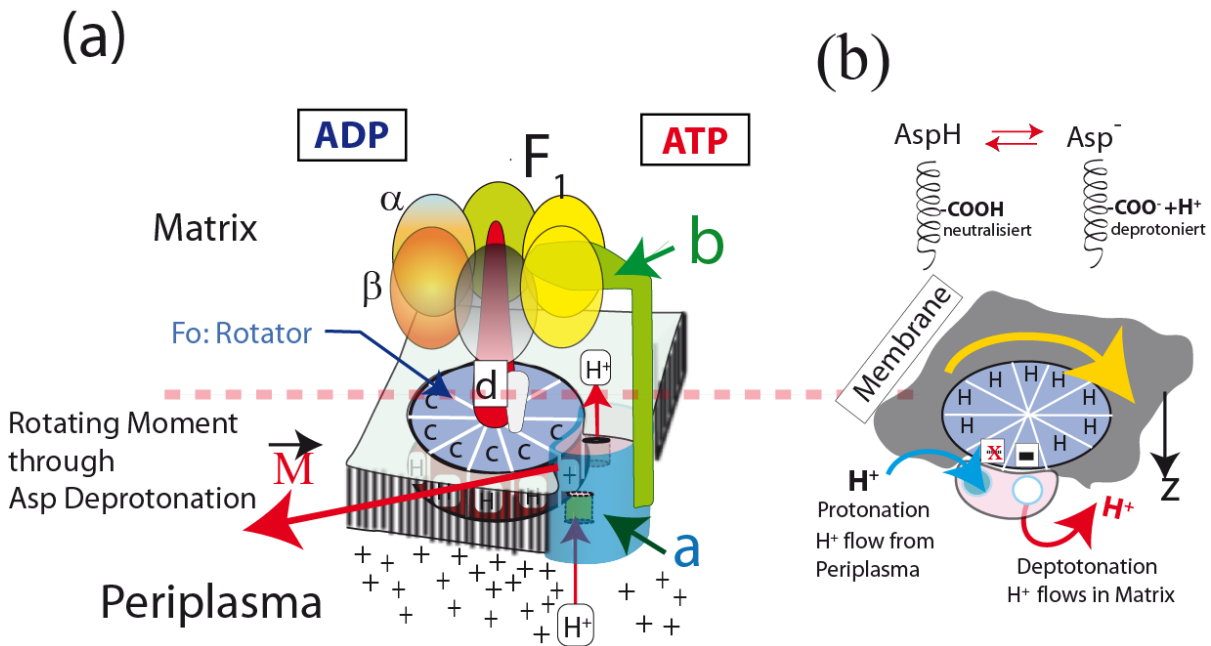


Figure 6:

(a) **Design of ATP-Synthase (MG 500 000Dalton) consisting of Rotor F0 and Stator F1.** F1 is made up of three dimers (α - β) which are connected to the membrane-embedded rotor F0 by the clamp b. The rotor consists of a ring of 10-14 proteins (c) coupled to the central socket (d). It is connected to the integral membrane protein a by the clamp b which interacts with the α , β dimers of F1. The membrane-penetrating section of b exhibits two half channels through which protons can flow to the aspartic acid and protonate this amino acid. The cyclic influx of protons to the left channel and the outflux from the right opening produces the angular momentum which drives the rotation of the F0 with respect to F1 (see discussion of Figure 5b).

(b) **Birds view on rotation motor in direction F0 \rightarrow F1, viewed from periplasm.** Note that charged Asp^- is expelled from the hydrophobic region of the membrane, while the protonated is attracted.

The most outstanding property of the F0/F1-ATPase is that it acts as synthesis machine generating ATP from ADP if the proton density is higher in the periplasm than in the matrix, but acts as ATP driven rotating motor if the H^+ -gradient is reversed. The function of the ATP synthesis is well described in textbooks of biochemistry and the reader interested in details of this process is referred to [Berg 2003] or the beautiful experiments of Dietz et al. [Dietz2004] and Rondelez et al. [Rondelez 2005]. We have now a closer look at the present understanding of molecular mechanism of the motor function since a very similar principle governs the force generation of rotating motors of bacteria discussed below (see Figure 7). A major role is played by the clamp c and the

two half channels marked by two sets of arrows. One penetrates from the periplasmic site and the other from the matrix side. Both end at the center at a site of the membrane penetrating α -helix which exposes an aspartic acid. Let us start from a resting state where both side chains of the amino acid are dissociated. This would be the case if the proton concentration in the periplasm and the matrix are equal and low. The negative charge of the aspartic acid prevents the rotation of the motor since the α -helix it cannot enter the hydrophobic region of the membrane. If the proton concentration in the periplasm is increased, the aspartic acid at the right side in Figure 7b is protonated and neutralized. Therefore, the helix is attracted by the membrane covered area of the rotor which rotates by an angle of $360/14$ degrees. Now the α -helix of the right comes in contact with the half channel opening to the matrix and the COOH group of the aspartic acid is dissociated and enters the matrix space and a new rotational jump can begin.

Appendix C. Martensitic transition: A diffusionless solid state transition (named after the German metallurgist Martens). Martensitic-transitions play a key role in metallurgy. The most important example is the generation of very hard steel generated by rapid cooling of iron from a high temperature state (called austenite). Solid state transitions are mediated by non-diffusive local displacements of the crystal lattice. Resulting in a change of a new crystal structure by simply shearing the lattice along a crystal plane, as indicated in Figure A.1 for a 2D crystal.

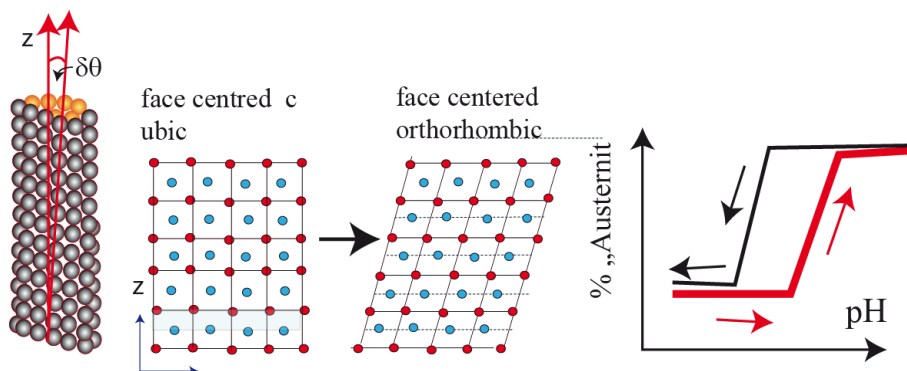


Figure A.1:

Martensitic transition from face centred two dimensional lattice from to face centred orthorhombic by shearin crystal along the horperpendicukarbto ztjhe cz-axis. In biological sysems the transition is triggered by pHchanges or The transitionexhibits a strong hysteresis which froms the baisi of memory alloys.